



Published in final edited form as:

Science. 2010 November 5; 330(6005): 841–845. doi:10.1126/science.1194637.

Fate Mapping Analysis Reveals That Adult Microglia Derive from Primitive Macrophages

Florent Ginhoux^{1,2,*}, Melanie Greter¹, Marylene Leboeuf¹, Sayan Nandi³, Peter See², Solen Gokhan⁴, Mark F. Mehler^{4,5}, Simon J. Conway⁶, Lai Guan Ng², E. Richard Stanley³, Igor M. Samokhvalov⁷, and Miriam Merad^{1,*}

¹Department of Gene and Cell Medicine and the Immunology Institute, Mount Sinai School of Medicine, 1425 Madison Avenue, New York, NY 10029, USA

²Singapore Immunology Network (SIgN), 8A Biomedical Grove, IMMUNOS Building Nos. 3–4, BIOPOLIS, 138648, Singapore

³Department of Developmental and Molecular Biology, Albert Einstein College of Medicine, 1300 Morris Park Avenue, Bronx, NY 10461, USA

⁴Institute for Brain Disorders and Neural Regeneration, Rose F. Kennedy Center for Research on Intellectual and Developmental Disabilities, and Department of Neurology, Albert Einstein College of Medicine, 1410 Pelham Parkway South, Bronx, NY 10461, USA

⁵Departments of Neuroscience, Psychiatry, and Behavioral Sciences, Albert Einstein College of Medicine, 1410 Pelham Parkway South, Bronx, NY 10461, USA

⁶Herman B Wells Center for Pediatric Research, Indiana University School of Medicine, 1044 West Walnut Street, Indianapolis, IN 46202, USA

⁷Laboratory for Stem Cell Biology, Center for Developmental Biology (CDB), RIKEN Kobe, Kobe 6500047, Japan

Abstract

Microglia are the resident macrophages of the central nervous system and are associated with the pathogenesis of many neurodegenerative and brain inflammatory diseases; however, the origin of adult microglia remains controversial. We show that postnatal hematopoietic progenitors do not significantly contribute to microglia homeostasis in the adult brain. In contrast to many macrophage populations, we show that microglia develop in mice that lack colony stimulating factor-1 (CSF-1) but are absent in CSF-1 receptor-deficient mice. In vivo lineage tracing studies established that adult microglia derive from primitive myeloid progenitors that arise before embryonic day 8. These results identify microglia as an ontogenically distinct population in the mononuclear phagocyte system and have implications for the use of embryonically derived microglial progenitors for the treatment of various brain disorders.

Copyright 2010 by the American Association for the Advancement of Science; all rights reserved.

*To whom correspondence should be addressed. Miriam.Merad@mssm.edu (M.M.); Florent_ginhoux@immunol.a-star.edu.sg (F.G.).

Supporting Online Material

www.sciencemag.org/cgi/content/full/science.1194637/DC1

Materials and Methods

Figs. S1 to S10

References

Movies S1 to S3

Although microglial ontogeny is an extensive area of research, much controversy remains regarding the nature of microglial progenitors (1, 2). The most consensual hypothesis to date is that embryonic and perinatal hematopoietic waves of microglial recruitment and differentiation occur in the central nervous system (CNS) (1, 2). However, the exact contribution of embryonic and postnatal hematopoietic progenitors to the adult microglial pool in the steady state remains unclear. We examined the contribution of primitive and definitive hematopoiesis to the adult microglial population that populates the CNS during normal development. Our results provide direct evidence that adult microglia derive from primitive myeloid progenitors that arise before embryonic day 8 (age E8.0) and for the predominant contribution of primitive myeloid progenitors to an adult hematopoietic compartment.

To address the contribution of perinatal circulating hematopoietic precursors to microglial homeostasis, we reconstituted sublethally irradiated C57BL/6 CD45.2⁺ newborns with hematopoietic cells isolated from CD45.1⁺ congenic mice (3). Although more than 30% circulating leukocytes and tissue macrophages were of donor origin 3 months after transplant (fig. S1A), 95% of adult microglia remained of host origin at this time point (fig. S1, A and B). These results suggest that, in contrast to previous reports (4, 5), perinatal circulating hematopoietic precursors, including monocytes, do not substantially contribute to adult microglial homeostasis. With use of adult congenic bone marrow chimera models, evidence in favor of (6–8) and against (9, 10) the contribution of circulating hematopoietic cells to microglial homeostasis has been proposed. We found consistently that 10 to 20% of microglia in the brain parenchyma are of donor origin at 10, 15, and 21 months after transplant (fig. S1C). Parabiotic mice, which share the same blood circulation, provide a means to follow the turnover of adult circulating hematopoietic precursors without the need for exposure to radiation injuries. Although the mixing of the myeloid lineage is less efficient than the mixing of the lymphoid lineage (11), an average of 30% of monocytes and tissue macrophages were donor-derived at 1 month and 12 months after parabiosis (fig. S1D) (12). In contrast, less than 5% of microglia were donor-derived at these time points (fig. S1D), in agreement with a previous report on 5-month-old parabionts (9). Consistent with previous reports (9, 10, 13), these results suggest that the recruitment of bone marrow-derived cells to the brain of chimeric animals is dependent on radiation-induced brain injuries that followed the transplantation regimen. These results also suggest that postnatal microglia are maintained independently of circulating monocytes throughout life and are maintained by local radio-resistant precursors that colonize the brain before birth.

Next, we examined the origin of microglia during development. In mouse embryos, the first wave of hematopoietic progenitors appears in the extra-embryonic yolk sac and leads to the production of primitive hematopoiesis, which takes place between E7.0 and E9.0 (14, 15). An independent wave of hematopoiesis termed “definitive hematopoiesis” is initiated within the embryo proper in the aorta, gonads, and mesonephros (AGM) region (14, 15). Around E10.5, hematopoietic progenitors start to colonize the fetal liver, which serves as a major hematopoietic organ after E11.5, whereas later during development hematopoiesis takes place in the spleen and bone marrow (15). Tissue macrophages in the adult are thought to derive from bone marrow monocytes, and the contribution of primitive hematopoiesis to adult tissue macrophages remains unclear (16). To determine the developmental stage at which the seeding of myeloid cells occurs in the brain, we used *Cx3cr1^{tgfp/+}* knockin mice (17) because the fractalkine receptor (CX3CR1) is a marker of early myeloid progenitors (18) and microglia (19). Consistent with previous results (20), myeloid cells expressing the hematopoietic marker CD45 and the adult macrophage/microglia markers CD11b, F4/80, and CX3CR1 were detectable in the developing brain starting from E9.5 (Fig. 1, A and B and fig S2). At E10.5, microglia cells were present in both the cephalic mesenchyme and the neuroepithelium, although at a lower density in the latter (Fig. 1A, fig. S2, and movies S1

and S2). The phenotype of microglial cells resembled that of yolk sac macrophages throughout embryonic development (Fig. 1, B and C, and fig. S3). Analysis of the DNA content of microglia and *in vivo* live imaging indicated that they were highly proliferative throughout embryonic life (fig. S4 and movie S3).

The differentiation of most macrophage populations in adult mice is controlled by colony stimulating factor-1 (CSF-1) and its receptor (CSF-1R) (21), but the role of the CSF-1 and CSF-1R in the development of yolk sac primitive macrophages and microglia is unknown. We found that CSF-1R was expressed in similar amounts on yolk sac macrophages and microglia at E9.5 (Fig. 2A). CSF-1R expression on microglia was maintained throughout development (Fig. 2A and fig. S5). Consistent with a requirement for CSF-1R expression, absence of CSF-1R greatly reduced the development of microglia (Fig. 2B and fig. S6A) and yolk sac macrophages (Fig. 2C and fig. S6B), whereas circulating monocytes were present in these mice (fig. S6, C and D). Furthermore, microglia remained largely absent throughout life in CSF-1R-deficient mice (Fig. 2B and fig. S6A). All together, these results suggest that the development of yolk sac macrophages and microglia, but not monocytes, is strongly dependent on CSF-1R. In contrast to many tissue macrophages, adult microglia can still form, albeit at reduced levels in *Csf-1^{op/op}* mice, which carry a natural null mutation of the *Csf-1* gene (22), but are absent in mice that lack CSF-1R (Fig. 2D). A second CSF-1R ligand, interleukin 34 (IL-34), has recently been identified in mice, humans (23), and birds (24). The expression of IL-34 mRNA in the brain is much higher than the expression of CSF-1 mRNA during early postnatal development and in the adult (25), consistent with an important role for IL-34 in the regulation of microglial homeostasis and with the increased severity of the microglial phenotype in *Csf-1^{r/-}* compared with *Csf-1^{op/op}* mice.

To examine the potential contribution of primitive myeloid precursors to adult microglia *in vivo*, we performed lineage tracing studies by using mice that express the tamoxifen-inducible *MER-Cre-MER* recombinase gene under the control of one of the endogenous promoters of the runt-related transcription factor 1 (*Runx1*) locus. Runx1 expression is first seen at E6.5 and is strongly up-regulated around E7.5 in the proximal visceral yolk sac region, and, until E8.0, Runx1⁺ cells are restricted to the extra-embryonic yolk sac and are absent from the embryo proper or allantois (26). We crossed the *Runx1-MERCre-MER* mice (*Runx1^{Cre/wt}*) with the Cre-reporter mouse strain *Rosa26^{R26R-eYFP/R26R-eYFP}* and induced recombination by a single injection of 4-hydroxytamoxifen (4' OHT) into pregnant females at different days of gestation. Active recombination in these knockin mice occurs in a small time window that does not exceed 24 hours postinjection (26) and leads to the irreversible expression of the enhanced yellow fluorescent protein (*eYFP*) reporter gene in Runx1⁺ cells and their progeny. At E10.5, embryos activated at E7.25 to E7.5 exhibited a similar proportion of labeled yolk sac macrophages and microglia [31% ± 10.8 (SE) for yolk sac macrophages and 32% ± 10.7 for brain progenitors, *n* = 10] (Fig. 3, A and B). The proportion of brain-infiltrating hematopoietic cells and microglia was similar in control littermate and heterozygote *Runx1^{Cre/wt}* embryos, suggesting that microglia homeostasis was not perturbed in *Runx1^{Cre/wt}* embryos (fig. S7, A and B). Furthermore, the proportion of eYFP⁺ microglia was similar in E10.5 and E13.5 embryos activated at E7.25 to E7.5 (fig. S7C), and within individual embryos the proportions of eYFP⁺ yolk sac macrophages and eYFP⁺ microglia were highly correlated (Fig. 3C). The partial labeling of Runx1⁺ yolk sac cells is inherent to *in vivo* labeling techniques and likely results from the insufficient expression of *MER-Cre-MER* and limited availability of the ligand in target cells (26). Thus, our model likely underestimates the contribution of Runx1⁺ precursors to adult microglia homeostasis, although we cannot exclude the potential contribution of nonlabeled precursors to this process. Nevertheless, these results strongly suggest that yolk sac macrophages and microglia have the same origin and that the first wave of microglia is specified before the end of E8.0. In adult mice activated at E7.25 to E7.5 (*n* = 10 from 3 litters), 32.11% ± 18.0

of microglia were also eYFP⁺ (Fig. 3D and fig. S8), a proportion similar to that of yolk sac macrophages and microglia found in E10.5 and E13.5 embryos activated at E7.25 to E7.5 (Fig. 3C and fig. S7). In contrast, less than 3% of blood circulating and tissue macrophages—including dermal and lung macrophages, as well as circulating T cells, B cells, and granulocytes—were eYFP⁺ in these mice (Fig. 3E and figs. S8 and S9). We also examined the earliest stage at which Runx1⁺ progenitors contributed to the adult microglial pool. In adult mice activated at E6.5 to E7.0, less than 3.77% ± 3.54 microglia were eYFP⁺, whereas 29.6% ± 10 microglia were eYFP⁺ in adult mice activated at E7.0 to E7.25 (Fig. 3E). In contrast 0.19% ± 0.26 and 0.09% ± 0.05 circulating leukocytes were eYFP⁺ in adult mice activated at E6.5 to E7.0 and E7.0 to E7.25, respectively (fig. S9). These results establish that primitive myeloid progenitors that arise before E7.5 contribute significantly to adult microglial homeostasis in the healthy brain but have limited potential to give rise to adult blood leukocytes.

To determine at which stage Runx1⁺ precursors or their progeny seed the brain during development, we injected *Runx1^{Cre/wt}; Rosa26^{R26R-LacZ}* pregnant females with a single dose of 4' OHT at E7.25 to E7.5 and traced the apparition of labeled cells into the brain rudiment at different time points after injection. A large number of Lac-Z⁺ cells populated the yolk sac of E8.5 embryos, whereas no labeled cells were detectable in the brain rudiment at this time point (Fig. 4A and fig. S10A). Brain-infiltrating cells appeared only when blood circulation developed, and a significant proportion of Lac-Z⁺ cells appeared associated with blood vessels and infiltrated the brain rudiment in E9.5 conceptus (Fig. 4B and fig. S10B). These results are consistent with prior findings showing that CSF-1R⁺ cells first accumulate in the yolk sac around E8.0 and infiltrate the embryo proper when blood vessels develop around E9.0 (27). To address whether the development of functional blood vessels was required for the recruitment of myeloid precursors into the brain rudiment, we used *Ncx-1^{-/-}* animals that lack a heartbeat and functional blood circulation because of a defect in sodium calcium exchanger 1 (28). We found that E9.5 to E10.5 *Ncx-1^{-/-}* embryos have yolk sac macrophages levels comparable or higher than control littermates (Fig. 4, C and E). In contrast, *Ncx-1^{-/-}* embryos have no detectable microglia in the brain, whereas *Ncx-1^{+/+}* control littermates already have a substantial number of microglia in the brain at this time-point (Fig. 4, D and E). Altogether, these results suggest that Runx1⁺ progenitors migrate from the yolk sac into the brain through blood vessels between E8.5 and E9.5.

To examine the contribution of definitive hematopoiesis to microglial homeostasis, we injected 4' OHT at E8.5, E9.5, and E10.5. The proportion of eYFP⁺ leukocytes known to derive from definitive hematopoiesis was much higher in mice activated at E8.5 and E9.5 compared with mice activated at E7.25 to E7.5 (up to 40% versus less than 3%, *n* = 10) (Fig. 3E and fig. S9). In contrast, few eYFP⁺ microglia were detected in the brains of adult mice activated after E8.5 and onward (Fig. 3E). The sharp descending contribution levels between E7.5 and E8.5 argue against the contribution of post-E7.5 Runx1⁺ anatomic locations to the labeling of the adult microglia lineage. Altogether, these data suggest minimal, if any, contribution of definitive hematopoiesis to the development of adult microglia.

Our results provide evidence that primitive myeloid precursors give rise to microglia residing in the adult CNS in the steady state. Primitive macrophages differentiate in the yolk sac of mammals, birds, and zebrafish before the onset of blood circulation (14). Studies in zebrafish revealed that yolk sac-derived macrophages spread in the cephalic mesenchyme before invading the brain through the pial surfaces and the fourth ventricle (29–31), findings consistent with the observation that microglia in humans are formed in the pia mater (32). The conservation of primitive macrophages throughout evolution implies that they serve an important role in the early embryo (14), most likely related to the clearance of apoptotic bodies and the normal remodeling of brain tissues. In contrast to most adult tissue

macrophages, microglia are maintained throughout life independently of any blood input and can resist high-dose γ -ray irradiation. Whether these primitive macrophages are uniquely suited to reducing the risk of inflammation-induced injuries and maintaining the CNS integrity throughout adult life will be important to determine.

The results of this study should help unravel the regulatory program that controls microglia differentiation and function in vivo and identify new means to manipulate microglia for the treatment of neural diseases.

Supplementary Material

Refer to Web version on PubMed Central for supplementary material.

Acknowledgments

We thank S. Nishikawa, H. Snoeck, and P. S. Frenette for intellectual input in the study; the RIKEN CDB Laboratory for Animal Resources and Genetic Engineering for providing the *Runx1-MER-Cre-MER* mice; G. Hoeffel, X. H. Zong, R. Basu and H. Ketchum for technical assistance; and L. Robinson for critical review and editing of the manuscript. This work was supported by NIH grants CA112100, HL086899, and AI080884 to M.M.; CA32551 and CA26504 to E.R.S.; and MH66290 and NS38902 to M.M. I.M.S. is supported by a grant from RIKEN Strategic Programs for Research and Development (President's Fund). M.G. is supported by the National Science Foundation of Switzerland. *Runx1-MER-Cre-MER* mice have CDB accession. no. CDB0524K (www.cdb.riken.jp/arg/mutant%20mice%20list.html).

References and Notes

1. Chan WY, Kohsaka S, Rezaie P. Brain Res. Brain Res. Rev. 2007; 53:344.
2. Ransohoff RM, Perry VH. Annu. Rev. Immunol. 2009; 27:119. [PubMed: 19302036]
3. Materials and methods are available as supporting material on *Science Online*.
4. Ling EA. J. Anat. 1979; 128:847. [PubMed: 489472]
5. Leong SK, Ling EA. Glia. 1992; 6:39. [PubMed: 1380949]
6. Lawson LJ, Perry VH, Gordon S. Neuroscience. 1992; 48:405. [PubMed: 1603325]
7. Priller J, et al. Nat. Med. 2001; 7:1356. [PubMed: 11726978]
8. Simard AR, Soulet D, Gowing G, Julien JP, Rivest S. Neuron. 2006; 49:489. [PubMed: 16476660]
9. Ajami B, Bennett JL, Krieger C, Tetzlaff W, Rossi FM. Nat. Neurosci. 2007; 10:1538. [PubMed: 18026097]
10. Mildner A, et al. Nat. Neurosci. 2007; 10:1544. [PubMed: 18026096]
11. Liu K, et al. Nat. Immunol. 2007; 8:578. [PubMed: 17450143]
12. Bogunovic M, et al. J. Exp. Med. 2006; 203:2627. [PubMed: 17116734]
13. Vallières L, Sawchenko PE. J. Neurosci. 2003; 23:5197. [PubMed: 12832544]
14. Lichanska AM, Hume DA. Exp. Hematol. 2000; 28:601. [PubMed: 10880746]
15. Orkin SH, Zon LI. Cell. 2008; 132:631. [PubMed: 18295580]
16. van Furth R, Cohn ZA. J. Exp. Med. 1968; 128:415. [PubMed: 5666958]
17. Jung S, et al. Mol. Cell. Biol. 2000; 20:4106. [PubMed: 10805752]
18. Liu K, et al. Science. 2009; 324:392. [PubMed: 19286519]
19. Harrison JK, et al. Proc. Natl. Acad. Sci. U.S.A. 1998; 95:10896. [PubMed: 9724801]
20. Alliot F, Godin I, Pessac B. Brain Res. Dev. Brain Res. 1999; 117:145.
21. Chitu V, Stanley ER. Curr. Opin. Immunol. 2006; 18:39. [PubMed: 16337366]
22. Blevins G, Fedoroff S. J. Neurosci. Res. 1995; 40:535. [PubMed: 7616613]
23. Lin H, et al. Science. 2008; 320:807. [PubMed: 18467591]
24. Garceau V, et al. J. Leukoc. Biol. 2010; 87:753. [PubMed: 20051473]
25. Wei S, et al. J. Leukoc. Biol. 2010; 88:495. [PubMed: 20504948]
26. Samokhvalov IM, Samokhvalova NI, Nishikawa S. Nature. 2007; 446:1056. [PubMed: 17377529]

27. Ovchinnikov DA, et al. *J. Leukoc. Biol.* 2008; 83:430. [PubMed: 17971498]
28. Koushik SV, et al. *FASEB J.* 2001; 15:1209. [PubMed: 11344090]
29. Sorokin SP, Hoyt RF Jr, Blunt DG, McNelly NA. *Anat. Rec.* 1992; 232:527. [PubMed: 1554104]
30. Herbomel P, Thisse B, Thisse C. *Dev. Biol.* 2001; 238:274. [PubMed: 11784010]
31. Herbomel P, Thisse B, Thisse C. *Development.* 1999; 126:3735. [PubMed: 10433904]
32. Cuadros MA, Navascués J. *Prog. Neurobiol.* 1998; 56:173. [PubMed: 9760700]

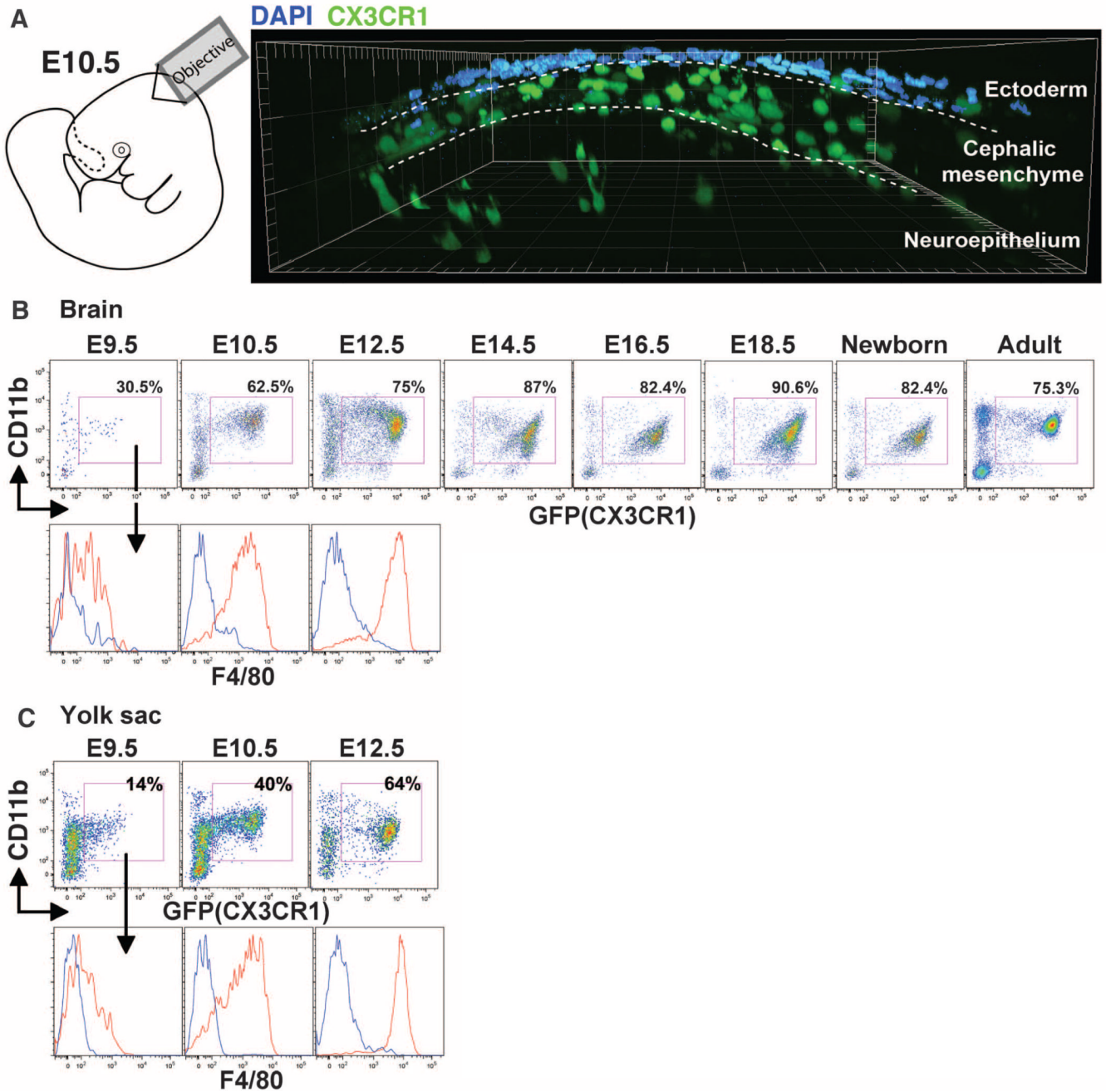


Fig. 1. Microglia arise during early embryonic life. (A) Left image, schematic of the imaging field. Right image, three-dimensional rendering of E10.5 brain rudiment from *Cx3cr1^{gfp/+}* mice. DAPI (blue) stains the ectoderm. Representative data of two experiments. (B and C) Flow-cytometric analysis of the expression of CD11b and GFP (CX3CR1) on gated 4',6'-diamidino-2-phenylindole (DAPI)-CD45⁺ brain (B) and yolk sac (C) cells isolated from *Cx3cr1^{gfp/+}* mice at different stages during development. Histograms show F4/80 (red) or isotype control (blue) on gated cells. Representative data of three experiments.

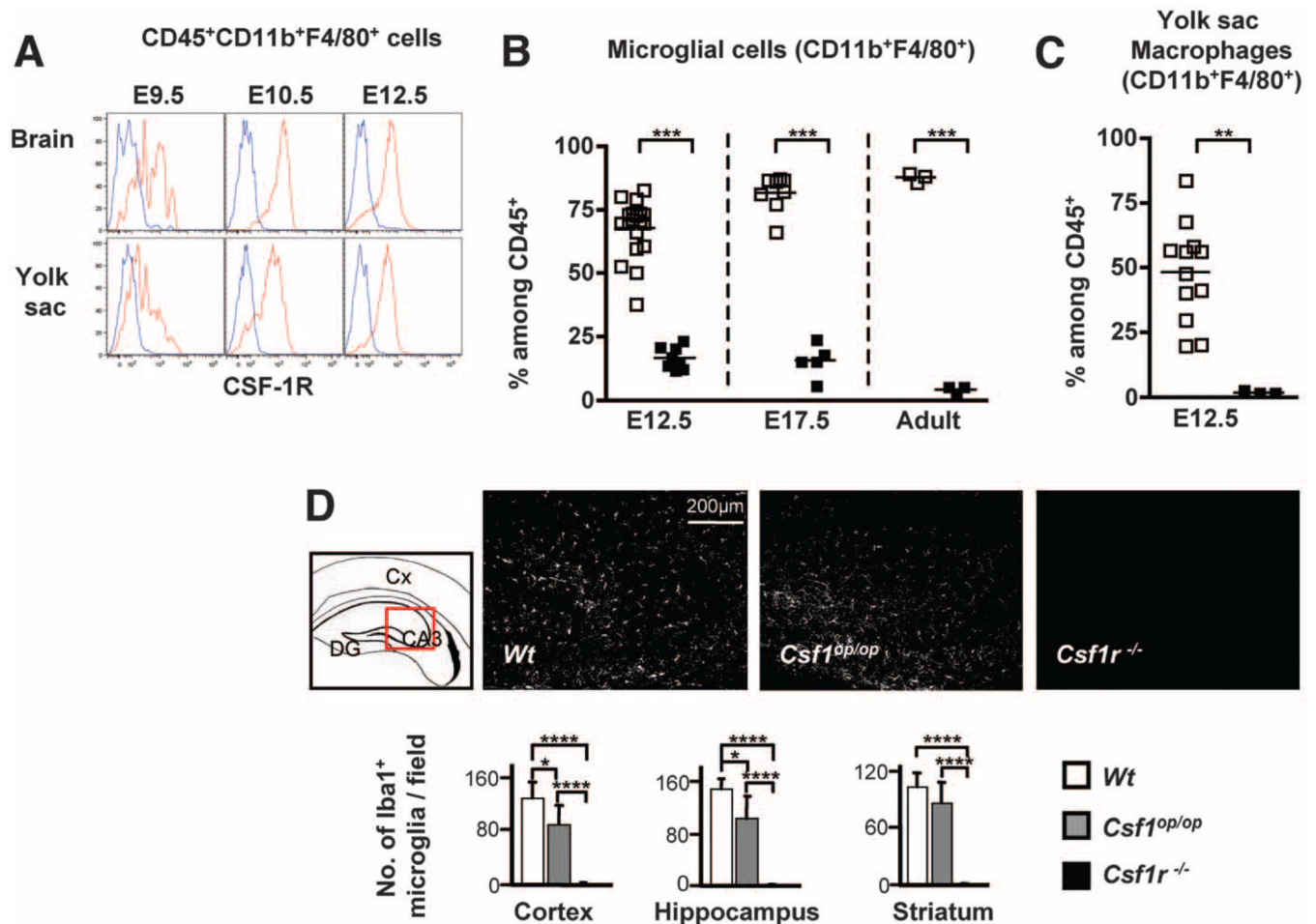


Fig. 2. Microglia and yolk sac macrophages are absent in *Csf1r*^{-/-} mice. **(A)** Flow-cytometric analysis of CSF-1R expression (red) on microglia and yolk sac macrophages (blue, isotype control). Representative data of three experiments. **(B and C)** Percentage of microglia **(B)** and yolk sac macrophages **(C)** in *Csf1r*^{-/-} (black squares) or control littermate (*Wt*) (white squares) FVB/NJ mice. Pooled data from three separate experiments. ***P* < 0.001; ****P* < 0.0001. **(D)** Coronal sections of 3-week-old *Wt*, *Csf1*^{op/op}, and *Csf1r*^{-/-} brains of region boxed in the schematic stained for the microglial marker Iba1. DG indicates dentate gyrus; Cx, cerebral cortex; CA3, CA3 region of the hippocampus. Mean number of Iba1⁺ cells per field from three different brain regions is shown. Average of six fields (0.5 mm²) per region per genotype. Error bars represent mean ± SD of data from two pooled experiments. **P* < 0.05; *****P* < 0.00001.

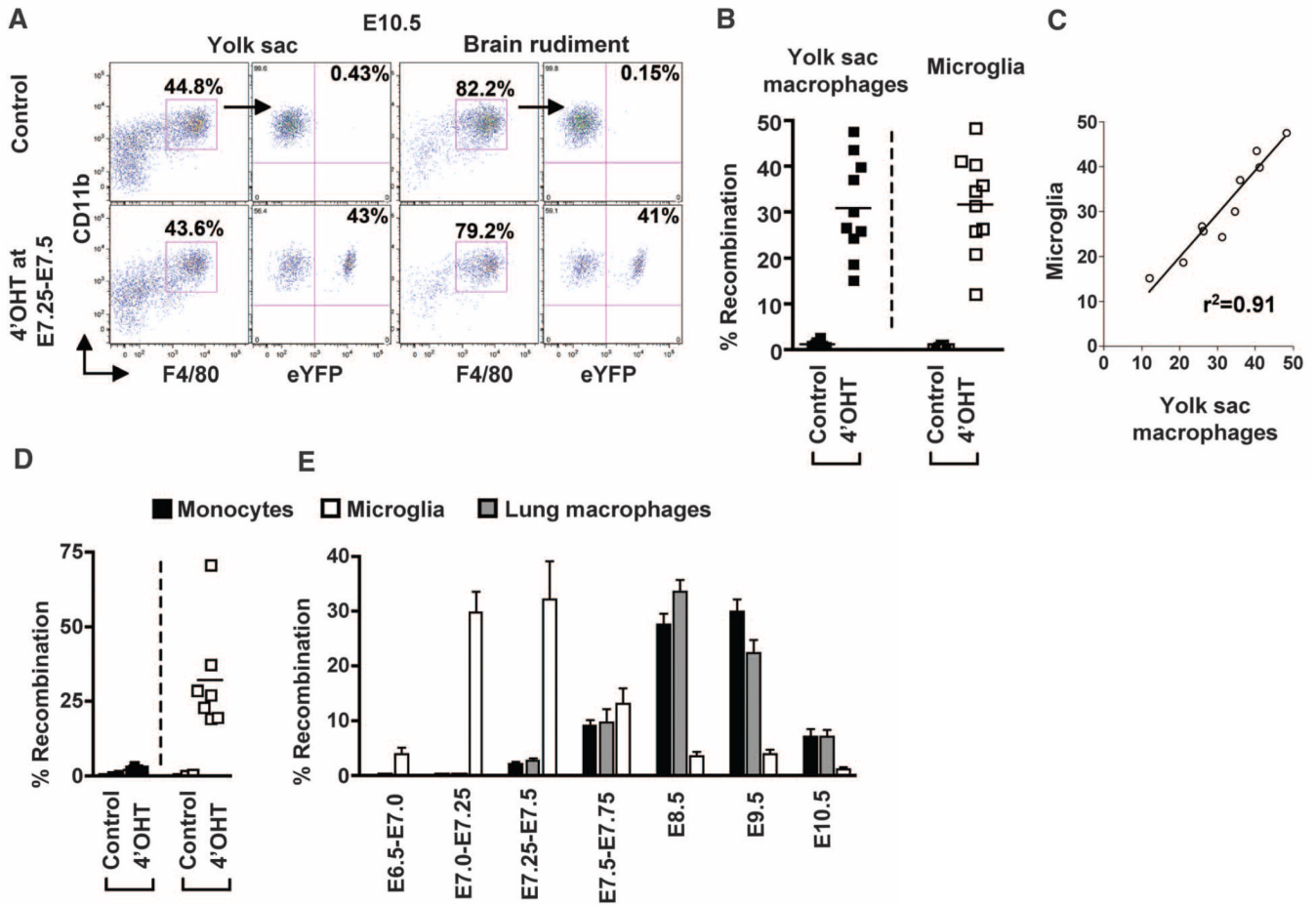


Fig. 3. Microglia arise from primitive myeloid progenitors. *Runx1^{Cre/wt}; Rosa26^{R26R-eYFP}* mice were treated with 4'OHT to induce Cre-mediated recombination at E7.25 to E7.5 and analyzed at E10.5 [(A) to (C)] or at 8 weeks postbirth [(D) and (E)]. Controls are nontreated mice. (A) Flow-cytometric analysis from one representative embryo showing the percent recombination among yolk sac macrophages and microglial progenitors. (B and D) Pooled data from two experiments showing the percent recombination among yolk sac macrophages and microglial progenitors cells in embryos (B), and among monocytes and microglia in adult mice ($n = 10$) (D). (C) Correlation and regression analysis between the percent recombination in microglial progenitors and yolk sac macrophages. r^2 , coefficient of regression. (E) Percent recombination among monocytes, lung macrophages, and microglia in adult mice activated at different embryonic age. Error bars represent mean \pm SEM of pooled data from two experiments ($n = 8$ to 16). Gating strategy for each leukocyte population is detailed in fig. S8.

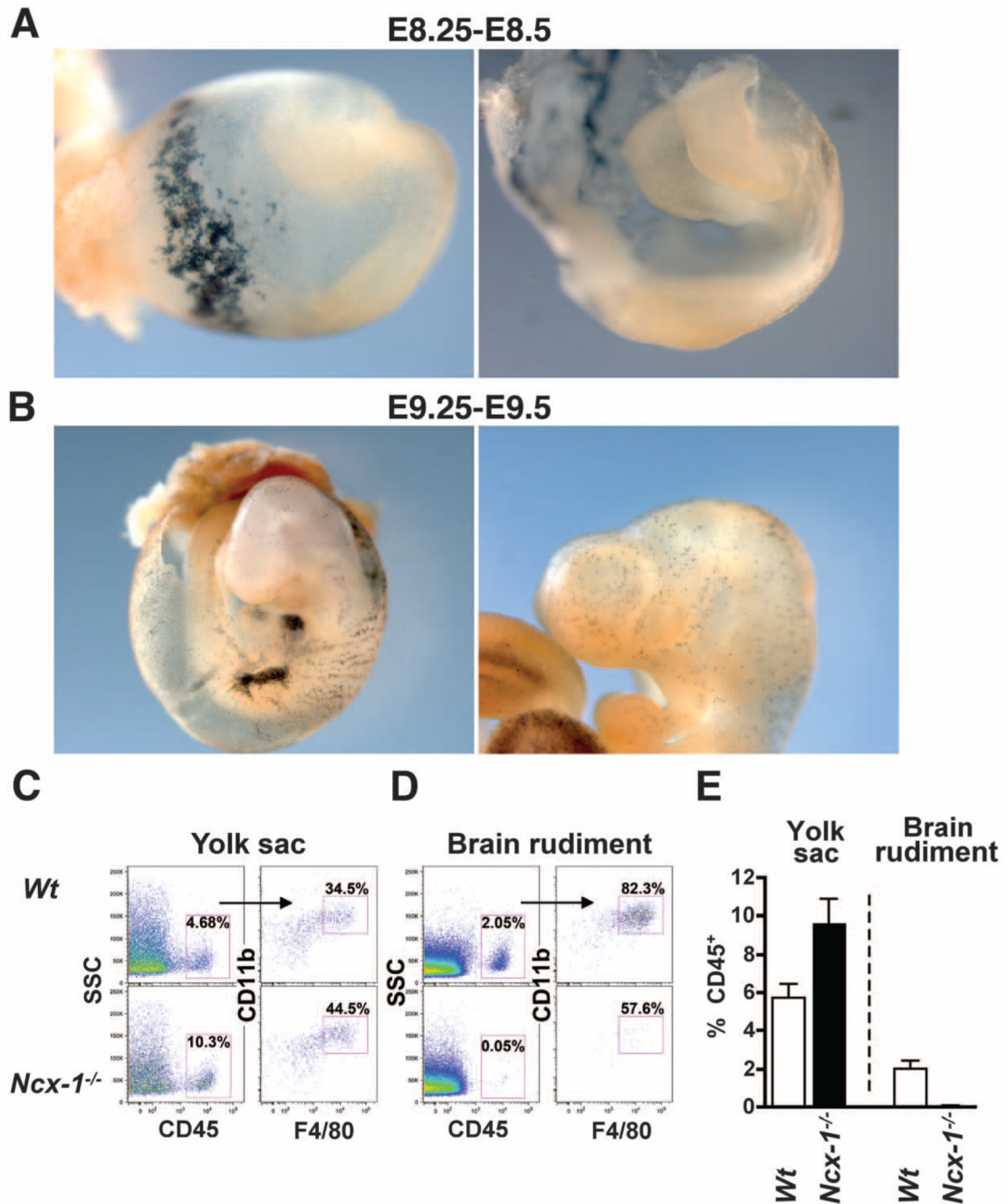


Fig. 4.

$Runx1^{+}$ yolk sac progenitors seed the brain between E8.5 and E9.5 through blood circulation. (**A** and **B**) *Runx1^{Cre/w}; Rosa^{26R26R-LacZ}* embryos activated at E7.25 to E7.5 were isolated at E8.25 to E8.5 (**A**) or E9.25 to E9.5 (**B**) and processed for whole-mount LacZ staining as described in the materials and methods section. At E8.25 to E8.5, labeled cells are detected in the yolk sac but not in the brain rudiment or in the neural tube (**A**), whereas labeled cells infiltrate the brain rudiment of E9.25 to E9.5 embryos (**B**). (**C** to **E**) Yolk sac and brain rudiment tissues were isolated from E10.0 to E10.5 *Ncx1*^{-/-} embryos or control littermates and processed for flow cytometry analysis as described in the materials and

methods section. Dot plots show the presence of yolk sac macrophages in *Ncx1*^{-/-} embryos and control littermates (C), whereas microglia were present in control but not in *Ncx1*^{-/-} embryos (D). (E) The percentage \pm SEM of hematopoietic cells (CD45⁺) in control littermates (white bars, $n = 4$) and *Ncx1*^{-/-} embryos (black bars, $n = 3$).